

Nonlinear transduction of emotional facial expression

Article

Accepted Version

Creative Commons: Attribution-Noncommercial-No Derivative Works 4.0

Gray, K. L.H. ORCID: <https://orcid.org/0000-0002-6071-4588>,
Flack, T. R., Yu, M., Lygo, F. A. and Baker, D. H. (2020)
Nonlinear transduction of emotional facial expression. *Vision Research*, 170. pp. 1-11. ISSN 0042-6989 doi:
<https://doi.org/10.1016/j.visres.2020.03.004> Available at
<https://centaur.reading.ac.uk/89417/>

It is advisable to refer to the publisher's version if you intend to cite from the work. See [Guidance on citing](#).

To link to this article DOI: <http://dx.doi.org/10.1016/j.visres.2020.03.004>

Publisher: Elsevier

All outputs in CentAUR are protected by Intellectual Property Rights law, including copyright law. Copyright and IPR is retained by the creators or other copyright holders. Terms and conditions for use of this material are defined in the [End User Agreement](#).

www.reading.ac.uk/centaur

CentAUR

Central Archive at the University of Reading

Reading's research outputs online



1 Nonlinear transduction of emotional facial expression

2 Katie L.H. Gray¹, Tessa R. Flack², Miaomiao Yu³, Freya A. Lygo³ & Daniel H. Baker^{3,4}

3 1. School of Psychology and Clinical Language Sciences, University of Reading, Reading, RG6

4 6BZ, UK

5 2. School of Psychology, University of Lincoln, Brayford Pool, Lincoln, LN6 7TS, UK

6 3. Department of Psychology, University of York, Heslington, York, YO10 5DD, UK

7 4. York Biomedical Research Institute, University of York, Heslington, York, YO10 5DD, UK

8 9 Abstract

10 To create neural representations of external stimuli, the brain performs a number of
11 processing steps that transform its inputs. For fundamental attributes, such as stimulus
12 contrast, this involves one or more nonlinearities that are believed to optimise the neural
13 code to represent features of the natural environment. Here we ask if the same is also true
14 of more complex stimulus dimensions, such as emotional facial expression. We report the
15 results of three experiments combining morphed facial stimuli with electrophysiological and
16 psychophysical methods to measure the function mapping emotional expression intensity to
17 internal response. The results converge on a nonlinearity that accelerates over weak
18 expressions, and then becomes compressive for stronger expressions, similar to the situation
19 for lower level stimulus properties. We further demonstrate that the nonlinearity is not
20 attributable to the morphing procedure used in stimulus generation. A preprint of this work
21 is available at: <https://doi.org/10.31234/osf.io/svw8q>

22 *Keywords:* emotional expressions; nonlinear transduction; SSVEP; psychophysics; morphing.

23

24 1. Introduction

25

26 Facial expressions are communicative tools; they signal an individual's emotional state and
27 motivation, and provide us with a wealth of information in social contexts (Adolphs, 2002;
28 Öhman, 2002). An expression can range from very subtle to very intense, and previous work
29 has used morphing software to parametrically manipulate emotional intensity within faces of
30 the same identity (Blair, Colledge, Murray, & Mitchell, 2001; Harris, Young, & Andrews, 2012;
31 Hess, Blairy, & Kleck, 1997). But how do changes in stimulus intensity map onto changes in
32 the brain's response to, and our perception of, another's face? Despite the importance of this
33 question for our understanding of perceived emotion, the precise mapping is currently
34 unclear.

35

36 Nonlinearities in the neural representation of low-level image features are very well
37 established. The brain responds to image contrast (defined as the luminance difference
38 between the brightest and darkest parts of an image, scaled by the mean luminance)
39 according to a saturating nonlinearity, that accelerates at intermediate contrasts, and
40 becomes shallow at higher contrasts. This pattern is consistent across measurements using
41 psychophysical contrast discrimination, matching and scaling paradigms (Kingdom, 2016;
42 Legge & Foley, 1980), functional magnetic resonance imaging (fMRI; Boynton, Demb, Glover,
43 & Heeger, 1999), electroencephalography (EEG; Campbell & Kulikowski, 1972; Tsai, Wade, &
44 Norcia, 2012), single- and multi-unit recording (Albrecht & Hamilton, 1982; Busse, Wade, &
45 Carandini, 2009; Ohzawa, Sclar, & Freeman, 1982) and optical imaging using voltage sensitive
46 dyes (Reynaud, Barthélemy, Masson, & Chavane, 2007).

47

48 Measuring neural responses to higher order stimulus properties (such as facial expression) is
49 possible using a fast periodic visual stimulation (FPVS) technique, which induces oscillations
50 in the EEG signal at specific frequencies. In this paradigm, ‘oddball’ target stimuli (e.g. faces
51 bearing an expression, or of a specific identity) are interleaved within a sequence of base
52 stimuli (e.g. neutral faces, or faces of a different identity) at a specific temporal frequency. If
53 the target can be discriminated, responses are evident at harmonics of the oddball frequency
54 (Braddick, Wattam-Bell, & Atkinson, 1986; Liu-Shuang, Norcia, & Rossion, 2014). Most
55 previous studies have used high intensity expressions and made comparisons across different
56 configurations (e.g. upright and inverted; Coll, Murphy, Catmur, Bird, & Brewer, 2019;
57 Dzhelyova, Jacques, & Rossion, 2017). However, by parametrically varying the intensity of
58 emotional expression in the oddball stimulus, an ‘emotion-response function’ (analogous to
59 a contrast-response function) can be measured. This directly reveals the transfer function
60 between facial expression intensity and neural response. One recent study (Leleu et al., 2018)
61 has reported such an experiment, and shown evidence of nonlinear components in the
62 emotion-response function.

63

64 The perceptual consequences of neural nonlinearities can also be measured in a variety of
65 ways. For stimulus levels around detection threshold, the slope of the psychometric function
66 (the function relating stimulus intensity to accuracy in a two-alternative-forced-choice
67 detection task) depends on the underlying transducer nonlinearity in that region of stimulus
68 space (assuming no uncertainty about the task). A linear system will result in a shallow
69 psychometric function (Weibull β values around 1.3, see Meese & Summers, 2012; Pelli, 1985;
70 Tyler & Chen, 2000), whereas accelerating nonlinearities produce steeper slopes. There is
71 some evidence from recent work (Marneweck, Loftus, & Hammond, 2013) of slopes with $\beta >$

72 1.3 for discriminating four distinct emotional expressions from neutral, though deviation from
73 linearity was not formally assessed.

74

75 A complementary approach to characterize signal processing is to use a discrimination
76 paradigm, in which a participant's ability to detect differences in magnitude is measured at a
77 range of starting ('pedestal') levels (Nachmias & Sansbury, 1974). Relative to detection in the
78 absence of a pedestal, weak pedestal levels can reduce the target level required to reach
79 threshold performance (facilitation), whereas strong pedestal levels can increase thresholds
80 (masking). The combination of these effects creates a characteristic 'dipper' shaped function
81 (Legge & Foley, 1980) when threshold is plotted against pedestal level, that is determined by
82 the gradient (steepness) of the underlying nonlinearity. A linear system would not produce
83 either the facilitation or masking effects, and thresholds should remain constant regardless
84 of pedestal level. Dipper functions have been reported for a range of sensory cues, including
85 motion (Gori, Mazzilli, Sandini, & Burr, 2011), blur (Watt & Morgan, 1983), depth (Georgeson,
86 Yates, & Schofield, 2008), texture (Morgan, Chubb, & Solomon, 2008), duration (Burr, Silva,
87 Cicchini, Banks, & Morrone, 2009), loudness (Raab, Osman, & Rich, 1963), and amplitude
88 modulation (Nelson & Carney, 2006), suggesting that the underlying nonlinearity is a common
89 property of perceptual systems.

90

91 One previous study has applied a similar paradigm to investigate the representation of facial
92 identity. Dakin and Omigie (2009) measured identity-strength discriminability of faces using
93 an odd-one-out paradigm. They morphed between an average identity face and a full identity
94 face in a number of steps. They then presented three faces: two identical faces (containing
95 the pedestal level of identity), and one face containing the pedestal identity with an additional

96 increment of identity. They repeated this at a number of different identity pedestal-levels,
97 measuring sensitivity at each level. When plotting threshold against pedestal identity, they
98 found evidence for shallow dipper-shaped functions, suggestive of a nonlinearity in the
99 representation of identity. However, these functions typically lacked the masking region
100 found for contrast (the dipper 'handle'). Work by Marenweck, Loftus and Hammond (2013)
101 reports discrimination for emotional expressions, but the pedestal level was not fixed within
102 a condition, making interpretation difficult. A primary aim of the present study is to
103 investigate whether emotional expression intensity is also subject to a process of nonlinear
104 transduction by measuring thresholds for expression discrimination at a range of pedestal
105 levels.

106

107 Here we report the results of three experiments. In the first we use an EEG paradigm to
108 measure neural responses to facial expressions in order to map out an emotion-response
109 function. In the second we measure the slope of the psychometric function for an expression
110 detection task. Finally, we assess the discriminability of emotional expressions from a range
111 of baseline (pedestal) levels. The results give a comprehensive picture of how expression
112 intensity information is processed to form an internal representation of others' emotional
113 states. We find evidence of a nonlinear transduction process similar to that reported for other
114 variables, which accelerates at low expression levels, and becomes shallower for more
115 intense expressions.

116

117 2. Methods

118

119 2.1 Participants

120

121 Twenty-four adult participants completed the EEG and detection experiments ($M_{\text{age}} = 23$; SD
122 = 5.29; 5 males), and six participants completed the discrimination experiment (1 male). All
123 had normal or corrected-to-normal visual acuity. All experiments were approved by the ethics
124 committee of the Department of Psychology at the University of York, and written informed
125 consent was obtained from all participants.

126

127 *2.2 Apparatus and stimuli*

128

129 All stimuli were derived from greyscale male and female faces taken from the NimStim face
130 set (Tottenham et al., 2009), depicting 6 basic emotional expressions (angry, fear, happy, sad,
131 surprise, and disgust; Ekman & Friesen, 1971). In the EEG and detection experiments, we used
132 16 female and 22 male identities, having a variety of racial backgrounds. For each identity, we
133 used a program (developed by Adams, Gray, Garner, & Graf, 2010) to morph between neutral
134 and an emotional expression in 6 steps, creating 7-levels of emotional intensity: 0, 6, 12, 24,
135 48, 96 and 144% (e.g. Calder et al., 2000; Calder, Young, Rowland, & Perrett, 1997). For the
136 discrimination experiment, we also created an averaged identity for each gender (based on
137 19 female and 23 male exemplars), and then morphed between neutral and 150% expression
138 in 0.5% steps. External features (i.e. hair and ears) were removed from all faces using an
139 elliptical mask blurred by a cosine function. All stimuli were equated for mean luminance and
140 root-mean-square contrast.

141

142 In the EEG experiment, brain activity was recorded from 64 scalp locations laid out according
143 to the 10/20 system in a WaveGuard cap (ANT Neuro, Netherlands). We also monitored blinks

144 through bipolar electro-oculogram electrodes placed above and below the left eye. Signals
145 were amplified and digitised at 1kHz and recorded using the ANT Neuroscan software (ANT
146 Neuro, Netherlands). Stimuli were presented using a gamma corrected VIEWPixx display
147 (VPixx Technologies Inc., Quebec, Canada) with a resolution of 1920x1200 pixels, a mean
148 luminance of 50cd/m², and a refresh rate of 120Hz, controlled by an Apple Macintosh
149 computer. Trigger codes were sent from the VIEWPixx device to the EEG amplifier using a 25-
150 pin parallel port to identify each condition and record stimulus onset times. The PsychToolbox
151 routines (Brainard, 1997) running in MATLAB were used to control the display hardware and
152 send triggers. The same display hardware was used in the detection experiment, but EEG
153 activity was not recorded. In the discrimination experiment, stimuli were centrally presented
154 on a gamma corrected 21-inch Iiyama VisionMaster Pro 510 monitor with a mean luminance
155 of 32cd/m² and a resolution of 1152x768 pixels, driven at 75Hz by an Apple Macintosh
156 computer.

157

158 *2.3 Procedures*

159

160 *EEG experiment:* Sequences of faces were presented for trials of 60 seconds duration. Faces
161 subtended approximately 8x12 degrees of visual angle at the viewing distance of 57cm, and
162 were presented against a grey background with a central black fixation cross. The contrast of
163 the faces was modulated between 0 and 100% according to a 5Hz sine wave (see Figure 1a).
164 The identity of the face was changed at the minimum of each period (when the contrast was
165 zero), resulting in a seamless stream of different identities. In this paradigm, each face
166 stimulus was presented for 200ms, but because contrast was 0 at the face onset and offset,
167 each face was visible for around 180ms. All stimuli had a neutral expression, except for an

168 'oddball' stimulus presented every fifth cycle (i.e. at 1Hz; see Figure 1a). This stimulus had a
169 randomly selected expression on each presentation, at a specific morph level that was
170 constant throughout the trial. Similar timings have been used previously with face stimuli (Liu-
171 Shuang et al., 2014; Rossion, Prieto, Boremanse, Kuefner, & Van Belle, 2012) and appear to
172 be a good compromise between potential floor and ceiling effects (i.e. too fast to allow
173 isolation of each individual response, or too slow to give large face-selective responses).
174 Participants were asked to fixate on a central cross for the duration of the trial and try to
175 minimise blinking; there was no behavioural task. Each block consisted of eight trials; one for
176 each morph level, plus an inversion condition using the 96% expression, but with all faces
177 rotated through 180 degrees. There was an inter-trial interval of 8 seconds. Each participant
178 completed four repetitions, taking around 40 minutes in total.

179

180 *Detection experiment:* We used a two-interval forced choice procedure that was designed to
181 closely mirror the temporal properties of the EEG experiment. Participants were presented
182 with two sequential streams of faces; a target stream containing a single emotional face
183 embedded within 8 neutral distractors, and a null stream containing only neutral faces. The
184 target face always appeared on the fifth cycle (the midpoint of the target stream; see Figure
185 1b). The target and distractors were random identities, and the same identity was never
186 repeated on two adjacent cycles. The two streams were separated by 500ms. Participants
187 were asked to detect which stream contained the emotional target, and indicated their
188 responses using a mouse. Target intensity, target expression, and target interval were
189 randomised across trials. There were 480 trials (60 per emotional intensity condition,
190 including 60 trials for the inversion condition at the 24% morph level), separated into 5 blocks,
191 taking around 40 minutes to complete.

192

193 *Discrimination experiment:* We used a two-interval forced choice procedure; on each trial, a
194 face (subtending 10x16 degrees at the viewing distance of 57cm) was presented centrally for
195 100ms in each of two intervals, separated by 400ms. One face had its expression set at the
196 pedestal level (the null stimulus; pedestal levels were 0, 15, 30, 45, 60 and 75%), the other
197 face had its expression set at the pedestal level plus an increment (the target stimulus).
198 Participants indicated which interval contained the face with the strongest expression
199 intensity (i.e. the target) using a mouse. In additional conditions, pedestal and target stimuli
200 were applied to different halves of the face; the results of these conditions will be reported
201 in a subsequent publication. Stimuli were surrounded by a black square, and divided
202 horizontally by a black line. The purpose of the black line was to mask luminance
203 discontinuities caused by combining upper and lower face halves from different expression
204 intensities in some conditions, and is consistent with standard composite effect procedures
205 (Rossion, 2013). The gender of the face was chosen randomly on each trial (with equal
206 probability), but was the same across the null and target intervals. The expression was
207 constant across the null and target intervals, but was chosen at random on each trial in the
208 main experiment. On each trial, the level of the target increment was selected using a
209 staircase procedure (three-down, one-up, step size of 2.5%) that terminated after the lesser
210 of 70 trials or 12 reversals. Participants received auditory feedback on the accuracy of each
211 response. The main experiment took around 4.5 hours to complete for each participant, and
212 consisted of around 8000-9000 trials per participant (of which around ¼ are reported here).
213 We also ran a control experiment for a restricted set of pedestal levels, in which the
214 expression was fixed within a block.

215

216 2.4 Data Analysis

217

218 *EEG experiment:* We took the Fourier transform of the EEG waveform (i.e. transformed the
219 responses from the time domain to the frequency domain) from each electrode for the 60
220 seconds during which stimuli were presented. There was a strong response from occipital
221 electrodes at the baseline frequency (5Hz) in all conditions, reflective of the general change
222 in contrast (and other image properties, such as identity) of the stimuli at this rate. Our
223 measure of interest was the amplitude at harmonics of the oddball frequency (1Hz), as this
224 measure is specific to emotional expression. To calculate the responses to the oddball stimuli,
225 we took the coherent average across repetitions and participants at 2, 3 and 4Hz, and then
226 averaged the amplitudes across these three frequencies to provide a single measure. We did
227 not include responses at 1Hz, as these were not distinguishable from the high noise levels in
228 this region of the spectrum (see Figure 1c), consistent with previous studies (Liu-Shuang et
229 al., 2014). We also excluded responses at and above the baseline frequency (≥ 5 Hz), as these
230 are difficult to interpret given the strong contribution from the baseline flicker component.

231

232 *Detection and discrimination experiments:* Individual thresholds were estimated from each
233 participant's responses (as well as the pooled data in the detection experiment) by fitting a
234 cumulative Weibull function using the *quickpsy* package in *R* (Linares & López-Moliner,
235 2016). We defined threshold as the morph intensity required to reach 81.6% correct (i.e. the
236 balance point of the Weibull function), and the slope as the β parameter of the fit.

237

238 *Data and code availability:* Primary analyses were performed in *R*. Analysis scripts and raw
239 data are available at: <http://dx.doi.org/10.17605/OSF.IO/8MS4Y>

240

241 3. Results

242

243 *3.1 The emotion-response function is nonlinear*

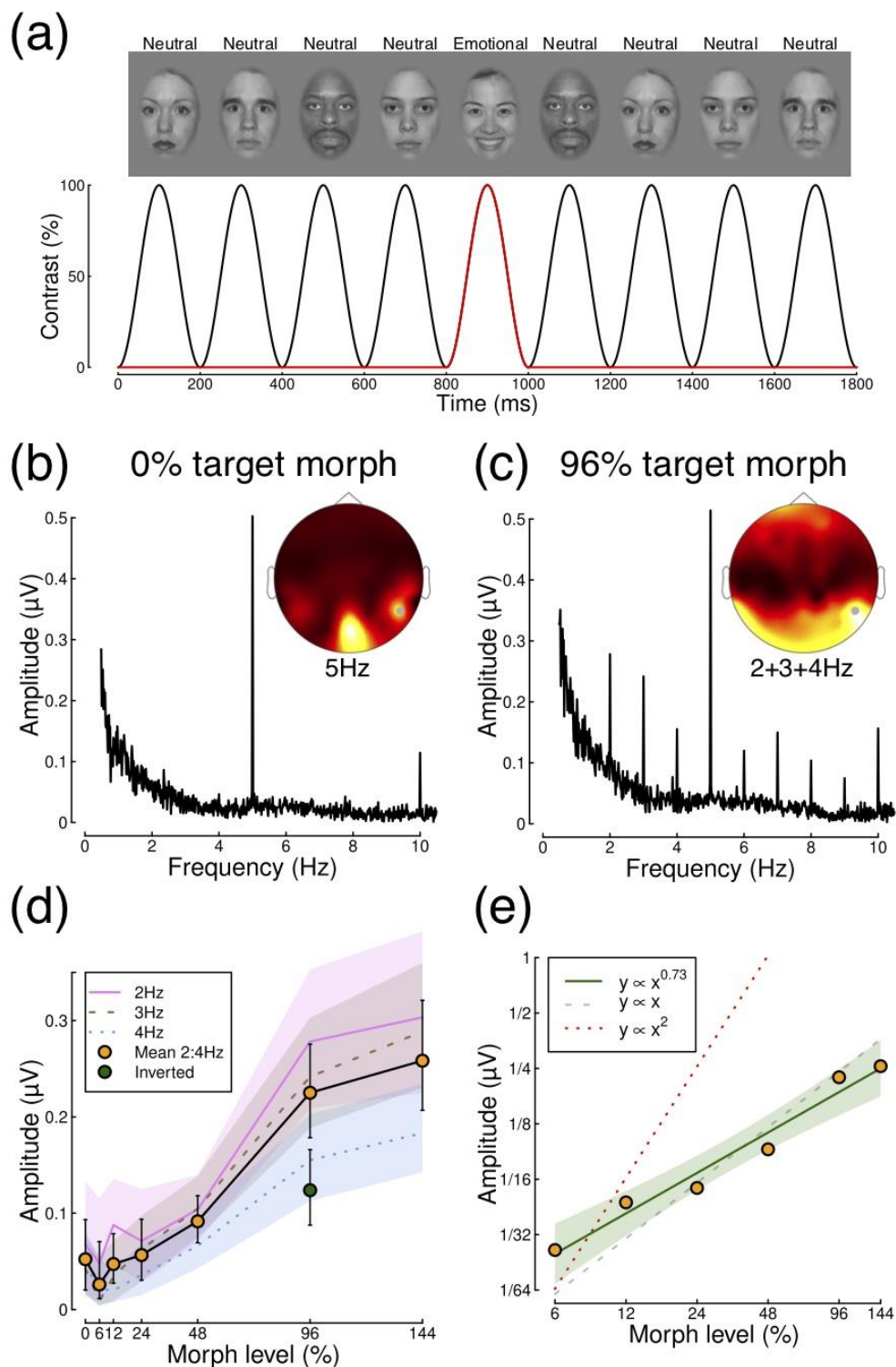
244

245 In our first experiment, we measured the neural response to stimuli of different emotional
246 intensities using a steady-state FPVS EEG paradigm, in a group of 24 adults. Streams of face
247 images with random identities were presented at 5Hz, with every fifth ‘oddball’ image bearing
248 a randomly chosen emotion, and the remainder being neutral (see Figure 1a). When the
249 oddball faces were also neutral (i.e. had a 0% expression morph level) there were clear
250 responses only at the carrier modulation frequency of 5Hz (see Figure 1b). When the oddball
251 faces carried a strong expression, responses were also evident at harmonics of the oddball
252 frequency (i.e. multiples of 1Hz, see Figure 1c), and were strongest over parieto-occipital
253 electrodes in the right hemisphere. These responses increased monotonically with morph
254 level at each of the first three harmonics (2, 3 and 4Hz), as shown by the lines in Figure 1d,
255 and their average (orange-filled circles in Figure 1d). Consistent with previous work
256 (Dzhelyova et al., 2017), inverting all images in the stream generated a much weaker
257 expression-specific response, as shown by the green symbol in Figure 1d (paired t-test; $t=5.29$,
258 $df=23$, $p=0.000023$, $d=1.1$, $BF=1025$).

259

260 To assess the linearity of these data, we replotted the average across the first three harmonics
261 on log-log axes (see Figure 1e). The best fit regression line to these data had a slope of 0.73,
262 and the upper bound of a bootstrapped 95% confidence interval on this slope estimate was

263 also below 1 (lower CI = 0.54; upper CI = 0.91). This is evidence of a compressive nonlinearity,
 264 equivalent to $y = x^{0.73}$, where x is morph level.



265

266 Figure 1: Neural SSVEP responses are lateralised and nonlinear. Panel (a) represents the stimuli presented during

267 a brief (1.8s) period of an extended (60s) trial. Stimulus contrast was sinusoidally modulated at 5Hz, with the

268 face image changed every 200ms at the trough of the modulation. An ‘oddball’ emotional face was presented
269 every 5 cycles, at a rate of 1Hz. Panel (b) shows the Fourier spectrum in the condition where the oddball stimuli
270 were also neutral, averaged across all participants (N=24). A strong response is evident at the modulation
271 frequency (5Hz), which is maximal at the occipital pole, with additional activity at more lateral sites. The
272 spectrum is derived from electrode P8, shown by the grey point. Panel (c) shows the Fourier spectrum for a 96%
273 target morph level. Here additional peaks in the spectrum are evident at integer frequencies. Panel (d) shows
274 emotion-response functions at individual frequencies (2, 3 and 4Hz) and their average (orange points). Shaded
275 regions and whiskers represent bootstrapped 95% confidence intervals across participants. Panel (e) shows the
276 average data replotted on log-log axes. Dashed and dotted lines show canonical predictions for a linear system
277 (dashed) and a squaring nonlinearity (dotted). The solid green line shows the best fit regression line in
278 logarithmic units, which has a slope of 0.73, with the green shaded region giving 95% confidence intervals of the
279 regression line.

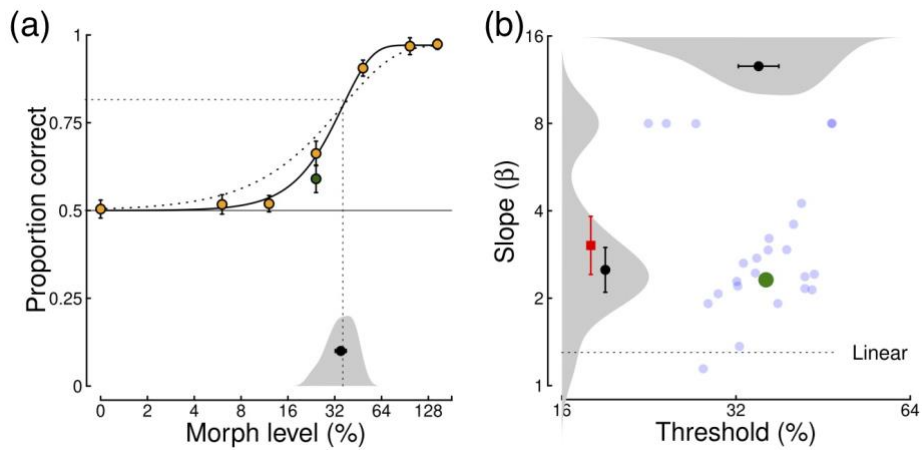
280

281 *3.2 A nonlinear psychometric function for emotion detection*

282

283 We next sought to measure the psychometric function for detection of emotional expressions
284 as a function of morph level. We based the stimulus sequence on that used in the SSVEP
285 experiment, and presented two sequences of 9 face images, each lasting 1.8 seconds (see
286 Figure 1a). One sequence comprised only neutral faces, and the other contained an emotional
287 face as the fifth image. Participants indicated which sequence they believed contained the
288 emotional face. Performance increased monotonically as a function of morph level, from
289 chance performance at low morph levels (0-12%), reaching near ceiling performance for
290 morph levels of 96 and 144% (see Figure 2a). Again, there was an inversion effect (see green
291 point in Figure 2a), which reduced accuracy from 0.66 to 0.59 when the faces were presented
292 upside-down (paired t-test; $t=3.19$, $df=23$, $p=0.004$, $d=0.65$, $BF=10.28$).

293



294

295 Figure 2: Nonlinear psychometric functions for detection of emotional expression. Panel (a) shows the group
 296 average psychometric function (N=24), along with the best fitting Weibull function (black solid curve). The grey
 297 shaded region at the foot shows the distribution of individual thresholds, along with the mean (black point). The
 298 black dotted curve is a Weibull function with the same threshold, but a slope of $\beta = 1.3$, showing the prediction
 299 for a linear system. Panel (b) shows individually fitted thresholds and slopes (blue points), along with the fit to
 300 the group average data (green). Grey shaded regions show distributions for each parameter, along with their
 301 means across participants (black points). For slope values, the red square is the mean with the 4 outliers at $\beta =$
 302 8 included, and the black point shows the mean with the outliers excluded. The dotted black line at $\beta = 1.3$ gives
 303 the prediction for a linear system. Error bars in both panels show 95% confidence intervals.

304

305 We fitted a cumulative Weibull function to the group averaged psychometric function (see
 306 solid curve in Figure 2a), and also to the functions for each individual participant (N=24), to
 307 estimate the threshold and slope. The group average threshold at 81.6% correct occurred at
 308 a morph level of 31.0%. This agreed well with the mean of the individual thresholds, which
 309 was 30.9%. The psychometric slope for the group averaged data was $\beta = 2.31$, substantially
 310 above the slope expected for a linear system of $\beta = 1.3$ (assuming no uncertainty). A
 311 psychometric function with a slope of $\beta = 1.3$ is shown by the dotted curve in Figure 2a, and
 312 is a poor fit to the data. Because slope values can sometimes be underestimated for group
 313 data if individual participants have different thresholds (see e.g. Wallis, Baker, Meese, &

314 Georgeson, 2013), we also assessed the slope values of individual fits (see Figure 2b). The
315 geometric mean psychometric slope across the group was $\beta = 2.9$, which was also above the
316 linear prediction of $\beta = 1.3$ ($t=7.42$, $df=23$, $p<0.001$, $d=1.51$, $BF=101258$). Four fits returned a
317 slope at the upper bound of the permitted values ($\beta = 8$). When these participants were
318 excluded, the geometric mean slope reduced to $\beta = 2.4$, which was still significantly steeper
319 than $\beta = 1.3$ ($t=8.88$, $df=19$, $p<0.001$, $d=1.98$, $BF=396167$).

320

321 The slope value of $\beta \approx 2.4$ corresponds to an effective transduction exponent of
322 approximately $2.4/1.3 = 1.85$. How can we reconcile this apparently accelerating nonlinearity
323 around detection threshold with the compressive nonlinearity implied by our EEG data? One
324 likely explanation is that the SSVEP paradigm was not sufficiently sensitive to detect
325 responses in the sub-threshold range of morph levels (morph levels below 48% did not
326 generate responses that were reliably above the noise floor, see Figure 1d). On the other
327 hand, psychophysical performance had almost asymptoted by this morph level (see Figure
328 2a). The two results can therefore be considered complementary, as they reveal the
329 nonlinearities operating in different ranges of the stimulus continuum. This is also consistent
330 with other cues, such as contrast, which feature an accelerating nonlinearity around
331 threshold and a compressive regime at higher stimulus intensities (e.g. Legge & Foley, 1980;
332 Meese, Georgeson, & Baker, 2006). This combination of nonlinearities should result in a
333 'dipper' function for emotional expression intensity discrimination; our final experiment
334 investigates this prediction.

335

336 *3.3 A 'dipper' function for emotion discrimination*

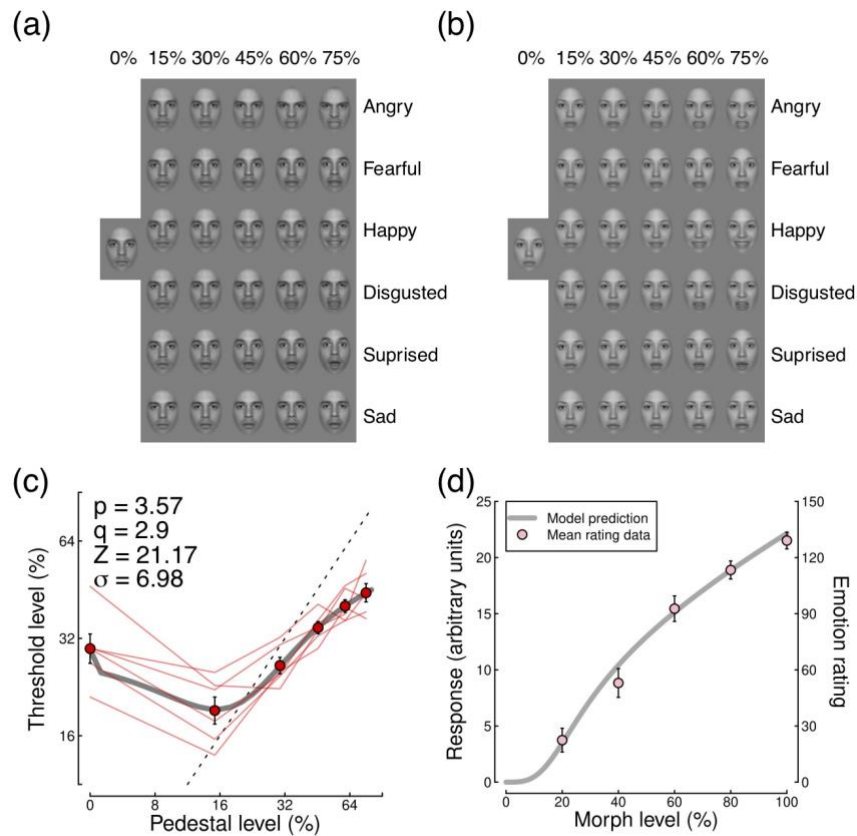
337

338 We measured emotion discrimination functions in six participants using a two-interval forced
339 choice paradigm. To avoid the potentially complicating factors of temporal and identity
340 uncertainty that might stem from the stimulus presentation sequences used in the previous
341 experiments, we simplified the paradigm in two ways. First, only a single face was presented
342 on each interval of a trial. Second, this face was an averaged identity, created by morphing
343 either male or female faces (see Figure 3a,b for examples). We measured discrimination at a
344 range of pedestal levels using a staircase method, and then fitted psychometric functions (see
345 Figure 2a) to estimate thresholds. A linear system should produce a completely flat function
346 for discrimination paradigms, where the pedestal level has no effect on threshold; any
347 modulation of thresholds is therefore evidence of nonlinear processing.

348

349 Thresholds at six pedestal morph levels are shown in Figure 3c. For a pedestal level of 0%, the
350 task is one of emotion detection. On average, participants required morph levels of around
351 29% to reliably detect (at 81.6% correct) the interval containing an emotional face (leftmost
352 point in Figure 3c). This compared closely with thresholds in the earlier experiment (mean of
353 31% morph level) using the method of constant stimuli with a different stimulus set and
354 temporal sequence. For weak pedestal expressions (15% morph level) sensitivity to the target
355 increment improved (i.e. thresholds decreased) by around a factor of 1.6, showing evidence
356 of facilitation from the pedestal. At higher pedestal levels a masking effect occurred, whereby
357 increment thresholds were higher than without a pedestal. This pattern was evident for each
358 individual participant (red lines in Figure 3c). Overall, there was a substantial effect of
359 pedestal level on threshold ($F(5,25)=23.49$, $p<0.001$, $\eta^2=0.75$, $BF=7758025$) that was driven
360 by thresholds in the 0% pedestal condition being significantly higher than in the 15% pedestal
361 condition ($t(5)=5.68$, $p=0.002$, $d=2.32$, $BF=20.72$), and lower than in the 60% and 75% pedestal

362 conditions ($t(5)=-3.33$, $p=0.021$, $d=1.36$, $BF=3.98$; $t(5)=-3.63$, $p=0.015$, $d=1.48$, $BF=5.06$,
 363 respectively). The slope of the rising limb of the dipper handle (estimated using linear
 364 regression over the highest four pedestal contrasts) was 0.57 (95% CIs: 0.41, 0.73).



365
 366 Figure 3: A dipper function for emotion discrimination. Panels (a,b) show example morphed facial stimuli for 6
 367 expressions at the pedestal morph levels, for male (a) and female (b) averaged identities. Panel (c) shows the
 368 emotion discrimination function for individual participants ($N=6$, red lines) and their average (points; error bars
 369 show $\pm 1SE$). The grey curve shows the best model fit (see text for details), and the dashed oblique line has unit
 370 slope. Panel (d) shows the underlying emotion response function implied by the model fitted to the data in (c).
 371 Pink points replot the averaged data of Hess et al. (1997).

372
 373 We fitted the average data with a standard nonlinear transducer function (Legge & Foley,
 374 1980) with four free parameters. The response to a face of a given intensity level (I) is given
 375 by,

376
$$f(I) = \frac{I^p}{Z^q + I^q}, \quad (1)$$

377

378 where p , q , and Z are free parameters. Thresholds are determined by calculating the
379 increment level that satisfies $f(\text{pedestal} + \text{increment}) = f(\text{pedestal}) + \sigma$, where σ is a further free
380 parameter that represents internal noise in the system. We determined best fitting
381 parameters using a downhill simplex algorithm that minimised the least-squares error
382 between data and model predictions. The best fitting curve is shown in Figure 3c, with
383 parameters in the upper left corner. With four free parameters, the model provides an
384 excellent description of the data, yielding an RMS error of 0.05dB.

385

386 In Figure 3d we plot the underlying transducer nonlinearity (the output of equation 1 for a
387 range of inputs) using the parameters derived from the fit in Figure 3c. The function has a
388 steep region around morph levels between 10% and 40% (i.e. around detection threshold),
389 but becomes shallower (compressive) at higher morph levels. This function represents the
390 way in which stimuli of different emotional intensities are mapped onto an internal response
391 scale, and shares several common features with the rating scale data of Hess et al. (1997),
392 most especially the shallowing at higher intensity levels. The points in Figure 3d replot the
393 data from Hess et al. (1997) averaged across expression (anger, disgust, happiness and
394 sadness) and face gender. It is clear that the data show extremely good correspondence with
395 the predictions of the model, with no additional free parameters required (though note that
396 the y-axes are scaled independently for the data points and the curve). In particular, the slope
397 of the function at high intensity levels accurately predicts that observed in the data.

398

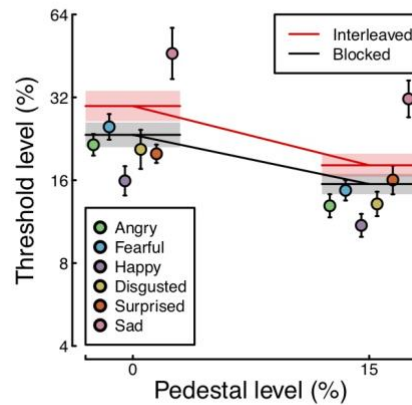
399 *3.4 Uncertainty reduction cannot explain the facilitation effect*

400

401 An alternative explanation for facilitation effects that does not require a nonlinear transducer
402 is uncertainty reduction (Pelli, 1985). Under this account, at detection threshold an observer
403 is uncertain about which mechanisms to monitor and performs poorly. When the pedestal is
404 added, this helps the observer determine which mechanisms (or features of the stimulus) to
405 attend to, and performance improves (facilitation). Because the facial expressions shown in
406 our experiments were determined randomly on each trial, we wondered if the facilitation
407 effects could be explained by expression uncertainty. To test this, we conducted a control
408 experiment (on five participants) in which we blocked trials by emotion. Participants were
409 explicitly told at the beginning of a block of trials which emotion would be presented. All other
410 experimental parameters were the same as for the main dipper experiment.

411

412 Results for this control experiment are presented in Figure 4. For all expressions, a facilitation
413 effect was still observed at 15% pedestal level. There were variations in sensitivity across
414 expressions (circles; see also Marneweck et al., 2013); in particular thresholds were
415 somewhat higher for sad expressions (pink symbols) than they were for other expressions.
416 The average thresholds from the blocked conditions (black lines) were slightly lower than
417 those from the interleaved method used in the main experiment (red lines). A 2 (pedestal
418 level) x 2 (blocking condition) ANOVA showed a main effect of pedestal level ($F(1,4)=47.79$,
419 $p=0.0023$, $\eta_p^2=0.92$) but no effect of blocking condition ($F(1,4)=3.63$, $p=0.13$) or interaction
420 effect ($F(1,4)=1.44$, $p=0.30$). We can therefore conclude that uncertainty effects were minimal
421 for our paradigm, and the dipper effect we report can be most straightforwardly explained
422 by a transducer nonlinearity.



423

424 Figure 4: Facilitation effects occur for individual emotional expressions. Circles show thresholds for individual
 425 emotions for the blocked control conditions, and the black horizontal bars give their average. The red horizontal
 426 bars represent analogous conditions from the main experiment for the five participants who completed the
 427 control experiment. Error bars and shaded regions show $\pm 1SE$ across participants (N=5).

428

429 4. Discussion

430

431 We have demonstrated a nonlinear mapping between the facial expression intensity in a
 432 stimulus and the internal response magnitude evoked by that stimulus. Across three
 433 experiments, we find that the nonlinearity is extremely similar to that reported for more basic
 434 visual dimensions such as contrast. Responses are negligible at low intensities, rise steeply at
 435 intermediate intensities around threshold, and exhibit a shallower, compressive portion at
 436 high intensities (Figure 3d). The nonlinearity produces facilitation and masking effects in an
 437 expression discrimination task, leading to a 'dipper' function similar to those reported for a
 438 range of other sensory cues, and accurately predicts rating data from a previous study.

439

440 What is the purpose of this nonlinear transduction process for expression intensity? One
441 explanation for similar phenomena in contrast transduction (e.g. contrast gain control;
442 Carandini & Heeger, 2012; Heeger, 1992) is that they focus the greatest sensitivity in the
443 region of intensities most commonly experienced in the environment, or that is of most use
444 to the organism. In everyday social interactions, individuals rarely display extremes of
445 emotion with the intensities associated with our 100% morphs (middle image in Figure 1a).
446 Instead, most of the expressions we encounter in real life are weaker, and perhaps quite
447 fleeting. Yet it is crucially important that we are able to detect and discriminate changes in
448 these expressions to gauge the emotional states of our conspecifics. Therefore a mechanism
449 that is most sensitive to changes in weak emotions is likely to have been most useful during
450 human evolution. It is also likely that adaptation to emotional expressions (e.g. Adams et al.,
451 2010; Butler, Oruc, Fox, & Barton, 2008; Fox & Barton, 2007; Juricevic & Webster, 2012;
452 Webster, Kaping, Mizokami, & Duhamel, 2004; Winston, Henson, Fine-Goulden, & Dolan,
453 2004) serves to maintain this sensitivity even when individuals display more extreme levels
454 of emotion on average.

455

456 The use of stimuli that are morphed along continua of expression or identity has become
457 increasingly common in face processing research. Yet some such studies implicitly assume
458 that linear steps in the morph space should correspond to linear differences in perception
459 (Blair et al., 2001; Orgeta & Phillips, 2008; Rotshtein, Henson, Treves, Driver, & Dolan, 2005).
460 Our data, along with those of others (Dakin & Omigie, 2009; Hess et al., 1997; Leleu et al.,
461 2018), indicate that this assumption is incorrect. Our decision to use a neutral expression as
462 a baseline condition was arbitrary (see Young et al., 1997), and we anticipate that similar
463 results would be obtained when morphing between two emotional expressions (see Chen,

464 Pan, & Chen, 2014 for preliminary evidence of this), or with other facial attributes associated
465 with character traits such as trustworthiness and dominance (Oosterhof & Todorov, 2008).
466 This suggests that multidimensional 'face space' accounts (e.g. Russell & Bullock, 1986;
467 Valentine, 1991) must become more complex than previously proposed, because of the need
468 to incorporate nonlinear processes that will distort the space (Tanaka, Giles, Kremen, &
469 Simon, 1998).

470

471 Category boundary effects for both emotional expression (Calder, Young, Perrett, Etcoff, &
472 Rowland, 1996; Etcoff & Magee, 1992) and facial identity (Beale & Keil, 1995) have been
473 widely reported, and can be considered a severe form of nonlinearity. Categorical processing
474 is typically defined by a rapid transition between categories (e.g. neutral and happy
475 expressions, or between two identities), and more similar perception or neural activity within
476 rather than between categories, even for comparable physical changes to the stimulus
477 (Rotshtein et al., 2005). We suspect our finding of a steep psychometric function for detection
478 (Figure 2), and a transducer that accelerates and then compresses (Figure 3d) might meet the
479 criteria often used for identifying categorical perception, and think it unlikely that our data
480 could discriminate between these two explanations. However, we note that category effects
481 are formally equivalent to high-threshold theory, which has been widely discredited for low-
482 level cues in favour of a signal detection theory approach (Nachmias, 1981; Tyler & Chen,
483 2000). Characterising the underlying nonlinearity, as we have done here, offers greater
484 explanatory and predictive power (e.g. Figure 3d) than positing a binary category boundary.

485

486 Alternatively, it may be that different brain regions contain categorical and continuous
487 representations of emotional expression, with evidence that cortical regions in the temporal

488 lobe contain a continuous representation, whereas subcortical structures including the
489 amygdala contain a categorical representation (Harris et al., 2012). Since subcortical
490 structures are too deep for EEG to probe directly, our SSVEP signals most likely originate in
491 cortical regions from which EEG activity can be detected, explaining the continuous response
492 we report (see Figure 1e). On the other hand, cortical responses might also relay activity from
493 subcortical regions, though presumably further processing would be applied in cortex that
494 might change the nature of the response.

495

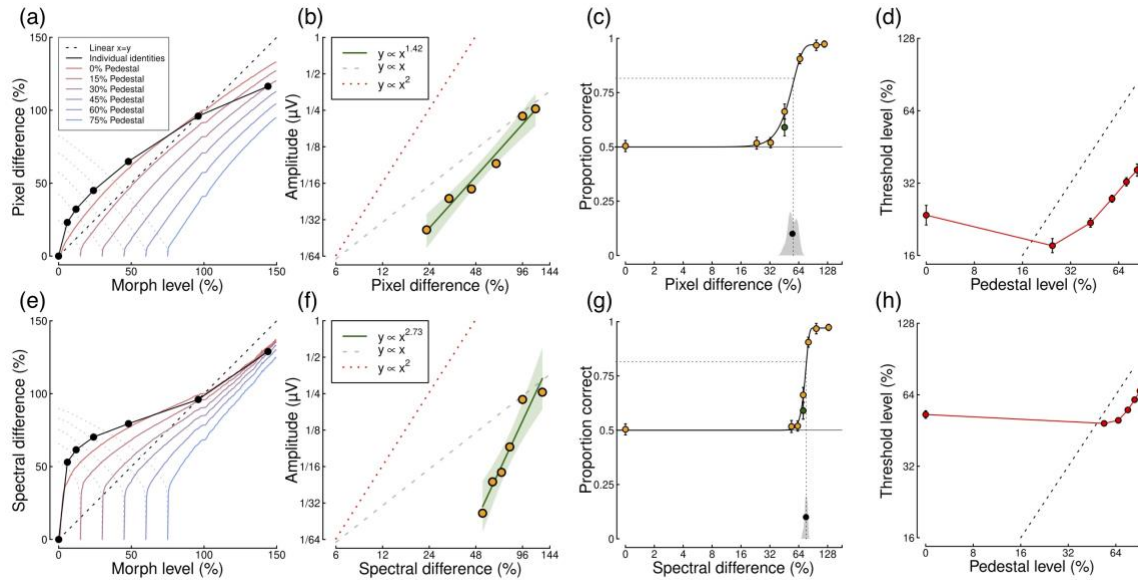
496 *4.1 Alternative metrics still support nonlinear processing*

497

498 In all our experiments we used a morphing technique to generate intermediate levels of
499 emotional expression. The morphing process produces a linearly increasing sequence of
500 expressions, but it manipulates the images geometrically in two dimensions, which could
501 introduce nonlinearities into the low level image features. In principle the apparently neural
502 nonlinearities we measure experimentally could be inherited from the stimuli if participant
503 responses were based on cues other than expression. We quantified this in two ways to
504 investigate whether image nonlinearities might be responsible for the apparently nonlinear
505 processing that we report. First, we measured the average absolute difference between pixels
506 in each successive morphed face image (the square root of the mean squared difference
507 produced a very similar result). This gives an aggregate measure of how local luminance
508 changes as a function of morph level, and shows evidence of a mild nonlinearity (see Figure
509 5a). Second, we measured the average absolute amplitude difference at each orientation and
510 spatial frequency in the Fourier transform of the images. This gives an indication of how the

511 global spectral content of the images changes as a function of morph level, and shows a more
 512 profound nonlinearity (see Figure 5e).

513



514

515 Figure 5: Alternative metrics still support nonlinear processing. Panels (a,e) show how stimuli of different morph
 516 levels differ in pixel luminance or Fourier amplitude. Black points show the estimates averaged across the 38
 517 identities used in the first two experiments. Coloured curves show the estimates averaged across the male and
 518 female examples used in the discrimination experiment, starting at different pedestal levels. In each case, the
 519 values were divided by the difference at 100% (or 96%) morph level and expressed as a percentage, so that the
 520 units were comparable to the morph level units used throughout the paper. The oblique dashed line shows the
 521 expectation for a linear mapping between units. The remaining panels replot the data from Figures 1e, 2a and
 522 3c using the alternative units, but with the same plotting conventions as described in the relevant figure
 523 captions.

524

525 To understand how these alternative metrics might influence our conclusions, we re-ran our
 526 analyses replacing the (linear) morph levels with the pixel or spectral difference values
 527 (rescaled to be in analogous percentage units). Our rationale is that if the nonlinearity in the
 528 stimulus is responsible for (some of) the apparently nonlinear processing in the brain, using

529 these alternative units will result in more approximately linear processing. These results are
 530 shown in Figure 5, and in Table 1 we report four indices of nonlinearity across the three
 531 experiments. Figures 5a,e show how the difference metrics change as a function of morph
 532 level. If these were entirely linear all curves would run parallel to the oblique dashed unity
 533 line. Clearly there are some substantial deviations, however we note that the very steep
 534 portion of the nonlinearity is at small morph levels (<15%) well below detection threshold
 535 (see Figure 2a) where neural responses cannot be differentiated from noise (Figure 1d). This
 536 means that the main influence of using these alternative units will be determined by the
 537 shallower slope evident at higher morph levels.

538

539 Table 1: Summary of indices of nonlinearity for different candidate input units. The units summarise the main
 540 features of nonlinearity for each experiment, and comprise: the slope of the emotion response function
 541 (determined by linear regression on log-log values), the transducer exponent inferred by the slope of the
 542 psychometric function (Weibull $\beta/1.3$), the amount of facilitation given by the ratio of thresholds between 0%
 543 and 15% morph levels of the dipper function, and the slope of the dipper handle (over the four highest pedestal
 544 levels). These indices give evidence of nonlinear processing when they deviate from the linear predictions listed
 545 in the bottom row.

546

Input units	SSVEP slope	Weibull $\beta/1.3$	Facilitation	Handle
Morph level	0.73	1.78	1.55	0.57
Pixel difference	1.42	3.42	1.34	0.76
Spectral difference	2.73	9.95	1.09	0.90
<i>Linear prediction</i>	1	1	1	0

547

548 When using the pixel difference metric, the emotion response function (Figure 5b) and the
549 psychometric function (Figure 5c) are shifted to the right and become steeper. This is because
550 over most of the range of stimulus levels the pixel differences increase with a slope of less
551 than 1 (compare points in Figure 5a with the oblique dashed line). This means that, relative
552 to using the morph level units, a smaller change in the stimulus is required to produce a unit
553 increase in response (or accuracy). The summary indices shown in Table 1 support this – the
554 slope of the emotion response function and the psychometric function both increase relative
555 to those derived using morph level units. The dipper functions also shift to the right and
556 become somewhat steeper, for similar reasons (see Figure 5d). However, the form of the
557 dipper is still apparent, with clear facilitation (a factor of 1.34), and masking in the ‘handle’
558 region (with a slope of 0.76). All of these changes become more extreme for the spectral
559 difference metric (Figure 5f-h), yet in all cases there is still evidence of nonlinear processing
560 in the brain. Overall then, our main indices of nonlinearity are changed somewhat by the use
561 of image-based units, but we can still conclude that neural processing of emotion is nonlinear.

562

563 We think it relatively unlikely that these low-level image differences are actually used by
564 participants for several reasons. In the psychophysical tasks, participants were explicitly
565 instructed to respond to the emotional content of the stimulus rather than image features
566 such as luminance, spatial frequency and orientation. Viewing the stimuli used in these
567 experiments delivers a compelling subjective experience of changes in emotion, which ‘pop
568 out’ of the dynamic sequences used in the first two experiments (see Figure 1a). Because we
569 used random identities in this temporal sequence, this will likely confound the low-level
570 changes that might be present within an identity. In addition, we observed strong inversion
571 effects (Eimer & Holmes, 2002; Yin, 1969) in the SSVEP and detection experiments (green

572 points in Figures 1d and 2a). For inverted stimuli, differences in low level image properties
573 remain constant, yet performance and neural responses are both significantly reduced
574 relative to upright stimuli. Finally, making reliable judgements about expression in everyday
575 life is unlikely to be possible using cues such as luminance, which will vary idiosyncratically
576 depending on the situation. It is conceivable that the visual system might use some of the
577 information from lower level features in combination with the expression information, yet
578 our analysis suggests that this would only increase the evidence for nonlinear neural
579 processing.

580

581 *3.3 Conclusions*

582

583 Across three experiments using different paradigms and stimuli, we find evidence that facial
584 expression intensity is processed in a nonlinear fashion. These findings are consistent with
585 the idea that relatively weak expressions are most typically experienced in everyday life, and
586 the brain might benefit from increasing sensitivity to subtle changes of expression within this
587 range. We predict that similar nonlinearities might apply along other dimensions of face-
588 space, including facial identity, age, attractiveness, and facial features that communicate
589 character traits such as dominance and trustworthiness. Such nonlinearities would distort the
590 geometry of 'face space' in predictable ways that might be quantified in future studies using
591 the methods developed here.

592

593 **5. Acknowledgements**

594

595 We thank Mike Burton and Andy Young for helpful comments on earlier versions of this work.

596 MY was supported by a bursary from the Experimental Psychology Society.

597

598

599

600 6. References

601

602 Adams, W. J., Gray, K. L. H., Garner, M., & Graf, E. W. (2010). High-level face adaptation
603 without awareness. *Psychological Science, 21*(2), 205–210.

604 <https://doi.org/10.1177/0956797609359508>

605 Adolphs, R. (2002). Recognizing emotion from facial expressions: psychological and

606 neurological mechanisms. *Behavioral and Cognitive Neuroscience Reviews, 1*(1), 21–

607 62. <https://doi.org/10.1177/1534582302001001003>

608 Albrecht, D. G., & Hamilton, D. B. (1982). Striate cortex of monkey and cat: contrast

609 response function. *Journal of Neurophysiology, 48*(1), 217–237.

610 <https://doi.org/10.1152/jn.1982.48.1.217>

611 Beale, J. M., & Keil, F. C. (1995). Categorical effects in the perception of faces. *Cognition,*

612 *57*(3), 217–239.

613 Blair, R. J., Colledge, E., Murray, L., & Mitchell, D. G. (2001). A selective impairment in the

614 processing of sad and fearful expressions in children with psychopathic tendencies.

615 *Journal of Abnormal Child Psychology, 29*(6), 491–498.

616 Boynton, G. M., Demb, J. B., Glover, G. H., & Heeger, D. J. (1999). Neuronal basis of contrast

617 discrimination. *Vision Research, 39*(2), 257–269.

618 Braddick, O. J., Wattam-Bell, J., & Atkinson, J. (1986). Orientation-specific cortical responses
619 develop in early infancy. *Nature*, *320*(6063), 617–619.
620 <https://doi.org/10.1038/320617a0>

621 Brainard, D. H. (1997). The Psychophysics Toolbox. *Spatial Vision*, *10*(4), 433–436.

622 Burr, D., Silva, O., Cicchini, G. M., Banks, M. S., & Morrone, M. C. (2009). Temporal
623 mechanisms of multimodal binding. *Proceedings. Biological Sciences*, *276*(1663),
624 1761–1769. <https://doi.org/10.1098/rspb.2008.1899>

625 Busse, L., Wade, A. R., & Carandini, M. (2009). Representation of concurrent stimuli by
626 population activity in visual cortex. *Neuron*, *64*(6), 931–942.
627 <https://doi.org/10.1016/j.neuron.2009.11.004>

628 Butler, A., Oruc, I., Fox, C. J., & Barton, J. J. S. (2008). Factors contributing to the adaptation
629 aftereffects of facial expression. *Brain Research*, *1191*, 116–126.
630 <https://doi.org/10.1016/j.brainres.2007.10.101>

631 Calder, A. J., Rowland, D., Young, A. W., Nimmo-Smith, I., Keane, J., & Perrett, D. I. (2000).
632 Caricaturing facial expressions. *Cognition*, *76*(2), 105–146.

633 Calder, A. J., Young, A. W., Perrett, D. I., Etcoff, N. L., & Rowland, D. (1996). Categorical
634 Perception of Morphed Facial Expressions. *Visual Cognition*, *3*(2), 81–118.
635 <https://doi.org/10.1080/713756735>

636 Calder, A. J., Young, A. W., Rowland, D., & Perrett, D. I. (1997). Computer-enhanced emotion
637 in facial expressions. *Proceedings. Biological Sciences*, *264*(1383), 919–925.
638 <https://doi.org/10.1098/rspb.1997.0127>

639 Campbell, F. W., & Kulikowski, J. J. (1972). The visual evoked potential as a function of
640 contrast of a grating pattern. *The Journal of Physiology*, *222*(2), 345–356.

641 Carandini, M., & Heeger, D. J. (2012). Normalization as a canonical neural computation.
642 *Nature Reviews. Neuroscience*, 13(1), 51–62. <https://doi.org/10.1038/nrn3136>

643 Chen, P.-Y., Pan, Y.-C., & Chen, C. C. (2014). The role of upper and lower faces in
644 discrimination happy and sad facial expressions. *IPerception*, 5(4), 340 [abstract].

645 Coll, M.-P., Murphy, J., Catmur, C., Bird, G., & Brewer, R. (2019). The importance of stimulus
646 variability when studying face processing using fast periodic visual stimulation: A
647 novel “mixed-emotions” paradigm. *Cortex; a Journal Devoted to the Study of the*
648 *Nervous System and Behavior*, 117, 182–195.
649 <https://doi.org/10.1016/j.cortex.2019.03.006>

650 Dakin, S. C., & Omigie, D. (2009). Psychophysical evidence for a non-linear representation of
651 facial identity. *Vision Research*, 49(18), 2285–2296.
652 <https://doi.org/10.1016/j.visres.2009.06.016>

653 Dzhelyova, M., Jacques, C., & Rossion, B. (2017). At a Single Glance: Fast Periodic Visual
654 Stimulation Uncovers the Spatio-Temporal Dynamics of Brief Facial Expression
655 Changes in the Human Brain. *Cerebral Cortex (New York, N.Y.: 1991)*, 27(8), 4106–
656 4123. <https://doi.org/10.1093/cercor/bhw223>

657 Eimer, M., & Holmes, A. (2002). An ERP study on the time course of emotional face
658 processing. *Neuroreport*, 13(4), 427–431.

659 Ekman, P., & Friesen, W. V. (1971). Constants across cultures in the face and emotion.
660 *Journal of Personality and Social Psychology*, 17(2), 124–129.

661 Etcoff, N. L., & Magee, J. J. (1992). Categorical perception of facial expressions. *Cognition*,
662 44(3), 227–240. [https://doi.org/10.1016/0010-0277\(92\)90002-Y](https://doi.org/10.1016/0010-0277(92)90002-Y)

663 Fox, C. J., & Barton, J. J. S. (2007). What is adapted in face adaptation? The neural
664 representations of expression in the human visual system. *Brain Research*, *1127*(1),
665 80–89. <https://doi.org/10.1016/j.brainres.2006.09.104>

666 Georgeson, M. A., Yates, T. A., & Schofield, A. J. (2008). Discriminating depth in corrugated
667 stereo surfaces: facilitation by a pedestal is explained by removal of uncertainty.
668 *Vision Research*, *48*(21), 2321–2328. <https://doi.org/10.1016/j.visres.2008.07.009>

669 Gori, M., Mazzilli, G., Sandini, G., & Burr, D. (2011). Cross-Sensory Facilitation Reveals Neural
670 Interactions between Visual and Tactile Motion in Humans. *Frontiers in Psychology*,
671 *2*, 55. <https://doi.org/10.3389/fpsyg.2011.00055>

672 Harris, R. J., Young, A. W., & Andrews, T. J. (2012). Morphing between expressions
673 dissociates continuous from categorical representations of facial expression in the
674 human brain. *Proceedings of the National Academy of Sciences*, *109*(51), 21164–
675 21169. <https://doi.org/10.1073/pnas.1212207110>

676 Heeger, D. J. (1992). Normalization of cell responses in cat striate cortex. *Visual*
677 *Neuroscience*, *9*(2), 181–197.

678 Hess, U., Blairy, S., & Kleck, R. E. (1997). The intensity of emotional facial expressions and
679 decoding accuracy. *Journal of Nonverbal Behavior*, *21*, 241–257.
680 <https://doi.org/10.1023/A:1024952730333>

681 Juricevic, I., & Webster, M. A. (2012). Selectivity of face aftereffects for expressions and
682 anti-expressions. *Frontiers in Psychology*, *3*, 4.
683 <https://doi.org/10.3389/fpsyg.2012.00004>

684 Kingdom, F. A. A. (2016). Fixed versus variable internal noise in contrast transduction: The
685 significance of Whittle’s data. *Vision Research*, *128*, 1–5.
686 <https://doi.org/10.1016/j.visres.2016.09.004>

687 Legge, G. E., & Foley, J. M. (1980). Contrast masking in human vision. *Journal of the Optical*
688 *Society of America*, 70(12), 1458–1471.

689 Leleu, A., Dzhelyova, M., Rossion, B., Brochard, R., Durand, K., Schaal, B., & Baudouin, J.-Y.
690 (2018). Tuning functions for automatic detection of brief changes of facial expression
691 in the human brain. *NeuroImage*, 179, 235–251.
692 <https://doi.org/10.1016/j.neuroimage.2018.06.048>

693 Linares, D., & López-Moliner, J. (2016). quickpsy: An R Package to Fit Psychometric Functions
694 for Multiple Groups. *The R Journal*, 8(1), 122. <https://doi.org/10.32614/RJ-2016-008>

695 Liu-Shuang, J., Norcia, A. M., & Rossion, B. (2014). An objective index of individual face
696 discrimination in the right occipito-temporal cortex by means of fast periodic oddball
697 stimulation. *Neuropsychologia*, 52, 57–72.
698 <https://doi.org/10.1016/j.neuropsychologia.2013.10.022>

699 Marneweck, M., Loftus, A., & Hammond, G. (2013). Psychophysical Measures of Sensitivity
700 to Facial Expression of Emotion. *Frontiers in Psychology*, 4.
701 <https://doi.org/10.3389/fpsyg.2013.00063>

702 Meese, T. S., & Summers, R. J. (2012). Theory and data for area summation of contrast with
703 and without uncertainty: Evidence for a noisy energy model. *Journal of Vision*,
704 12(11), 9–9. <https://doi.org/10.1167/12.11.9>

705 Meese, Tim S., Georgeson, M. A., & Baker, D. H. (2006). Binocular contrast vision at and
706 above threshold. *Journal of Vision*, 6(11), 1224–1243. <https://doi.org/10.1167/6.11.7>

707 Morgan, M., Chubb, C., & Solomon, J. A. (2008). A “dipper” function for texture
708 discrimination based on orientation variance. *Journal of Vision*, 8(11), 9.1-8.
709 <https://doi.org/10.1167/8.11.9>

710 Nachmias, J. (1981). On the psychometric function for contrast detection. *Vision Research*,
711 21(2), 215–223. [https://doi.org/10.1016/0042-6989\(81\)90115-2](https://doi.org/10.1016/0042-6989(81)90115-2)

712 Nachmias, J., & Sansbury, R. V. (1974). Letter: Grating contrast: discrimination may be better
713 than detection. *Vision Research*, 14(10), 1039–1042.

714 Nelson, P. C., & Carney, L. H. (2006). Cues for masked amplitude-modulation detection. *The*
715 *Journal of the Acoustical Society of America*, 120(2), 978–990.

716 Öhman, A. (2002). Automaticity and the Amygdala: Nonconscious Responses to Emotional
717 Faces. *Current Directions in Psychological Science*, 11(2), 62–66.
718 <https://doi.org/10.1111/1467-8721.00169>

719 Ohzawa, I., Sclar, G., & Freeman, R. D. (1982). Contrast gain control in the cat visual cortex.
720 *Nature*, 298(5871), 266–268.

721 Oosterhof, N. N., & Todorov, A. (2008). The functional basis of face evaluation. *Proceedings*
722 *of the National Academy of Sciences*, 105(32), 11087–11092.
723 <https://doi.org/10.1073/pnas.0805664105>

724 Orgeta, V., & Phillips, L. H. (2008). Effects of age and emotional intensity on the recognition
725 of facial emotion. *Experimental Aging Research*, 34(1), 63–79.
726 <https://doi.org/10.1080/03610730701762047>

727 Pelli, D. G. (1985). Uncertainty explains many aspects of visual contrast detection and
728 discrimination. *Journal of the Optical Society of America. A, Optics and Image*
729 *Science*, 2(9), 1508–1532.

730 Raab, D. H., Osman, E., & Rich, E. (1963). Intensity Discrimination, the “Pedestal” Effect, and
731 “Negative Masking” with White-Noise Stimuli. *The Journal of the Acoustical Society*
732 *of America*, 35(7), 1053–1053. <https://doi.org/10.1121/1.1918653>

733 Reynaud, A., Barthélemy, F. V., Masson, G. S., & Chavane, F. (2007). Input-output
734 transformation in the visuo-oculomotor loop: comparison of real-time optical
735 imaging recordings in V1 to ocular following responses upon center-surround
736 stimulation. *Archives Italiennes De Biologie*, 145(3–4), 251–262.

737 Rossion, B. (2013). The composite face illusion: A whole window into our understanding of
738 holistic face perception. *Visual Cognition*, 21(2), 139–253.
739 <https://doi.org/10.1080/13506285.2013.772929>

740 Rossion, B., Prieto, E. A., Boremanse, A., Kuefner, D., & Van Belle, G. (2012). A steady-state
741 visual evoked potential approach to individual face perception: effect of inversion,
742 contrast-reversal and temporal dynamics. *NeuroImage*, 63(3), 1585–1600.
743 <https://doi.org/10.1016/j.neuroimage.2012.08.033>

744 Rotshtein, P., Henson, R. N. A., Treves, A., Driver, J., & Dolan, R. J. (2005). Morphing Marilyn
745 into Maggie dissociates physical and identity face representations in the brain.
746 *Nature Neuroscience*, 8(1), 107–113. <https://doi.org/10.1038/nn1370>

747 Russell, J. A., & Bullock, M. (1986). On the dimensions preschoolers use to interpret facial
748 expressions of emotion. *Developmental Psychology*, 22(1), 97–102.
749 <https://doi.org/10.1037/0012-1649.22.1.97>

750 Tanaka, J., Giles, M., Kremen, S., & Simon, V. (1998). Mapping attractor fields in face space:
751 the atypicality bias in face recognition. *Cognition*, 68(3), 199–220.

752 Tottenham, N., Tanaka, J. W., Leon, A. C., McCarry, T., Nurse, M., Hare, T. A., ... Nelson, C.
753 (2009). The NimStim set of facial expressions: judgments from untrained research
754 participants. *Psychiatry Research*, 168(3), 242–249.
755 <https://doi.org/10.1016/j.psychres.2008.05.006>

756 Tsai, J. J., Wade, A. R., & Norcia, A. M. (2012). Dynamics of normalization underlying
757 masking in human visual cortex. *The Journal of Neuroscience*, *32*(8), 2783–2789.
758 <https://doi.org/10.1523/JNEUROSCI.4485-11.2012>

759 Tyler, C. W., & Chen, C. C. (2000). Signal detection theory in the 2AFC paradigm: attention,
760 channel uncertainty and probability summation. *Vision Research*, *40*(22), 3121–3144.

761 Valentine, T. (1991). A unified account of the effects of distinctiveness, inversion, and race
762 in face recognition. *The Quarterly Journal of Experimental Psychology. A, Human*
763 *Experimental Psychology*, *43*(2), 161–204.

764 Wallis, S. A., Baker, D. H., Meese, T. S., & Georgeson, M. A. (2013). The slope of the
765 psychometric function and non-stationarity of thresholds in spatiotemporal contrast
766 vision. *Vision Research*, *76*, 1–10. <https://doi.org/10.1016/j.visres.2012.09.019>

767 Watt, R. J., & Morgan, M. J. (1983). The recognition and representation of edge blur:
768 evidence for spatial primitives in human vision. *Vision Research*, *23*(12), 1465–1477.

769 Webster, M. A., Kaping, D., Mizokami, Y., & Duhamel, P. (2004). Adaptation to natural facial
770 categories. *Nature*, *428*(6982), 557–561. <https://doi.org/10.1038/nature02420>

771 Winston, J. S., Henson, R. N. A., Fine-Goulden, M. R., & Dolan, R. J. (2004). fMRI-adaptation
772 reveals dissociable neural representations of identity and expression in face
773 perception. *Journal of Neurophysiology*, *92*(3), 1830–1839.
774 <https://doi.org/10.1152/jn.00155.2004>

775 Yin, R. K. (1969). Looking at upside-down faces. *Journal of Experimental Psychology*, *81*(1),
776 141–145. <https://doi.org/10.1037/h0027474>

777 Young, A. W., Rowland, D., Calder, A. J., Etcoff, N. L., Seth, A., & Perrett, D. I. (1997). Facial
778 expression megamix: tests of dimensional and category accounts of emotion
779 recognition. *Cognition*, *63*(3), 271–313.

